*Internal Combustion Engines and Powertrain Systems for Future Transport 2019 –
Institute of Mechanical Engineers, ISBN 978-0-367-90356-5*

The development and testing of a free-piston engine generator for hybrid electric vehicle applications

A.J. Smallbone, S. Roy, K.V. Shivaprasad, B. Jia, A.P. Roskilly

Department of Engineering, Durham University, Durham, UK

ABSTRACT

In this work, we present some of the first experimental results along with simulation results obtained in developing and testing a novel dual-piston free-piston engine generator (FPEG), designed for electric- vehicle (EV) range-extender or hybrid powertrain applications. The benefits of a high-efficiency, compact and lightweight design of the proposed range-extender are presented. The technical details and experimental set-up of a two-cylinder prototype and its instrumentation are also outlined. Results are presented for simulation and recent test programmes carried out across both 2-stroke and 4-stroke operational modes. The methods associated with engine control are detailed alongside key post-processed engine characteristics.

1 INTRODUCTION

Today's global energy production aims at cleaner production to preserve and protect environmental resources. In recent decades, the world has started to address the environmental changes caused by emissions of hydrocarbon fuelled vehicles and is instigating solutions to reduce these pollutants. Also, the faster depletion of fossil fuels has led to research on alternative fuel engines in replacing existing conventional fuels with a clean, economical and efficient energy source. To this end, the current perception is that conventional engines will be replaced by more electrified vehicle powertrains. The main challenge for electric vehicles (EVs) designers is limited driving range. One option is to have a small on-board installation of an electric generator such that the driving range can be increased. This has led to disruptive advancements in the development of range extenders. One such technology is the use of a free piston engine generator (FPEG).

The FPEG has the potential to be an effective integrated engine and electricity generator. The piston moves along the engine cylinder which is driven by combustion gases and kinetic energy of the piston movement is converted into electrical energy by a linear electric machine. When using a FPEG, the use of crank shaft and connecting rod is eliminated resulting in several advantages such as higher efficiency, compact design and piston motion is directly converted to electrical power; due to the simplicity of the system. Along with these, the compression ratio can be easily varied, and the stroke length is independent as there is no crankshaft. In a FPEG, the electrical energy is achieved from chemical energy by means of a combustion process.

In 1928, an engineer and inventor R.P Pescara from Argentina presented the free-piston engine (FPE) [1] and since several designs for free-piston engines have been projected. In all these designs, the piston is free to move between its endpoints which makes the free-piston engine to run with variable stroke length and high control requirements [2]. Zhang and Sun [3] stated that when seven renewable fuels like ethanol, biodiesel, hydrogen etc. are considered for trajectory-based combustion control enabled by FPEG, it was found that FPEG has the highest flexibility of fuel compared to others. The work of Roman Virsik [4] compared FPEG with other range extender technologies available and then has concluded that FPEGs with the use of ICEs (internal combustion engines) are feasible and has higher efficiencies with lower emissions and NVH values. This can be implemented in vehicles. Heron and Rinderknecht [5] in their work compared several range extender technologies for electric vehicles. They compared the FPEG, polymer electrolyte fuel cells, TRE (traditional reciprocating engine) and ICEs. They concluded that the FPEGs have higher efficiency compared to TREs and ICEs. In the 1940s, the German navy used the free-piston air compressors to supply compressed air for launching torpedoes. The free-piston engines were used to feed hot gas to a power turbine. This was employed in stationary and marine powerplants, most successful being a model developed by SIGMA in France [6].

Researchers at Toyota central laboratory, Japan, developed the FPEG prototype comprised of a linear generator, a gas spring chamber and two-stroke combustion chamber with hollow circular step shaped piston. In this study, the characteristics of FPEG motion were studied both numerically and experimentally for enabling stable continuous operation. In the simulation, the researchers evaluated the FPEG with SI and premixed charged compression ignition modes of combustion. The output power of 10kW was obtained with both combustion mode whereas premixed charged compression ignition mode of combustion delivered higher thermal efficiency of 42% compared to SI combustion mode. Experimental results confirmed that the FPEG prototype operated stably for quite a long period of time, despite of the abnormal combustion during the test. The researchers have explored the unique piston motion, which causes its impacts on combustion and power generation in the FPEG [7], [8]. The detailed review on free-piston engine on its history and development was presented by Hanipah, Mikalsen and Roskilly [9], [10].

Free-piston engines are broadly classified into three types based on piston arrangement as single piston, opposed piston and dual piston [11]. The working principle is identical for each type, but variances between them are the compression stroke realization and combustion chambers design. FPEGs consists of different modules. They are central combustion module, central gas spring module, central combustion with integrated gas spring module, central combustion with branched linear generators module and dual module system, either of which can be used according to the user. These modules are chosen accordingly based on their NVH behaviour. However, with the implementation of the FPEG the NVH is observed to be low. The engine noise and vibrations occur because of the mechanical forces, and combustion process can be controlled by synchronizing these modules. Due to the presence of higher degrees of freedom for the FPEG system, Homogenous Compression Ignition (HCCI) combustion can also be implemented [4].

This article presents the experimental outputs on FPEG prototype system based on a dual-piston free-piston engine design. This design and its operation is built upon a series of robust numerical modelling studies carried out over the years by the researchers of the centre [12], [13], [14], [15].

2 DESCRIPTION OF THE ENGINE CONFIGURATION

2.1 Dual-piston FPEG concept engine

The schematic configuration and prototype of FPEG established at the Sir Joseph Swan Centre for Energy Research is shown in schematic in Figure 1 and photos shown in Figure 2 respectively. This design of the engine generator is in accordance with the patent by Mikalsen and Roskilly [16]. The adopted design parameters are tabulated in Table 1. The FPEG concept mainly comprises two opposing internally combusted FPE and a linear electric machine. Each of the free-piston engine is consisted combustion chamber, spark plug, piston and set of poppet valves. The engine employs an actuated control system for intake and exhaust. The electric machine, generally called the stator, is located between the engines and it can be operated as a generator, or a motor. The pistons of FPEG are connected using moving part of the system called mover. The linear electric machine initiated the starting process by operating as a motor and then switched as generator mode once the system attains steady state. Combustion takes place alternatively in each cylinder of engines, which drives the piston and mover assembly to oscillate back and forth motion. The electric generator then converts the movement of the piston into electrical energy.

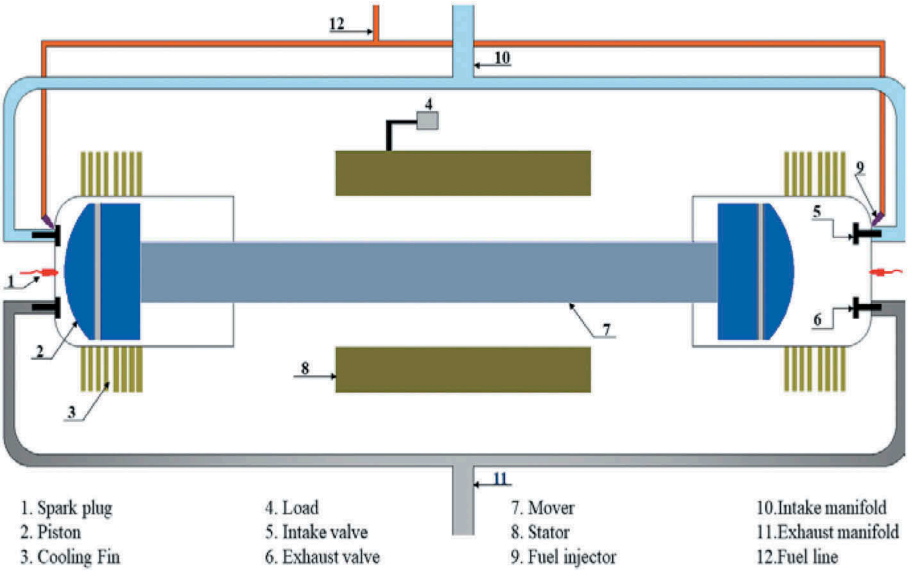

Figure 1. Schematic diagram of FPEG.

Table 1. Specifications of prototype FPEG.

Parameters	Value	Unit
Maximum stroke	40.0	mm
Cylinder bore	50.0	mm
Intake/exhaust valve lift	4.0	mm
Intake valve diameter	20.0	mm
Moving mass	7.0	kg
Exhaust valve diameter	18.0	mm
Intake manifold pressure	1.3	bar
Exhaust manifold pressure	1	bar
Ignition position from cylinder head	5.0	mm
Load constant of the generator	810	$N/(ms^{-1})$

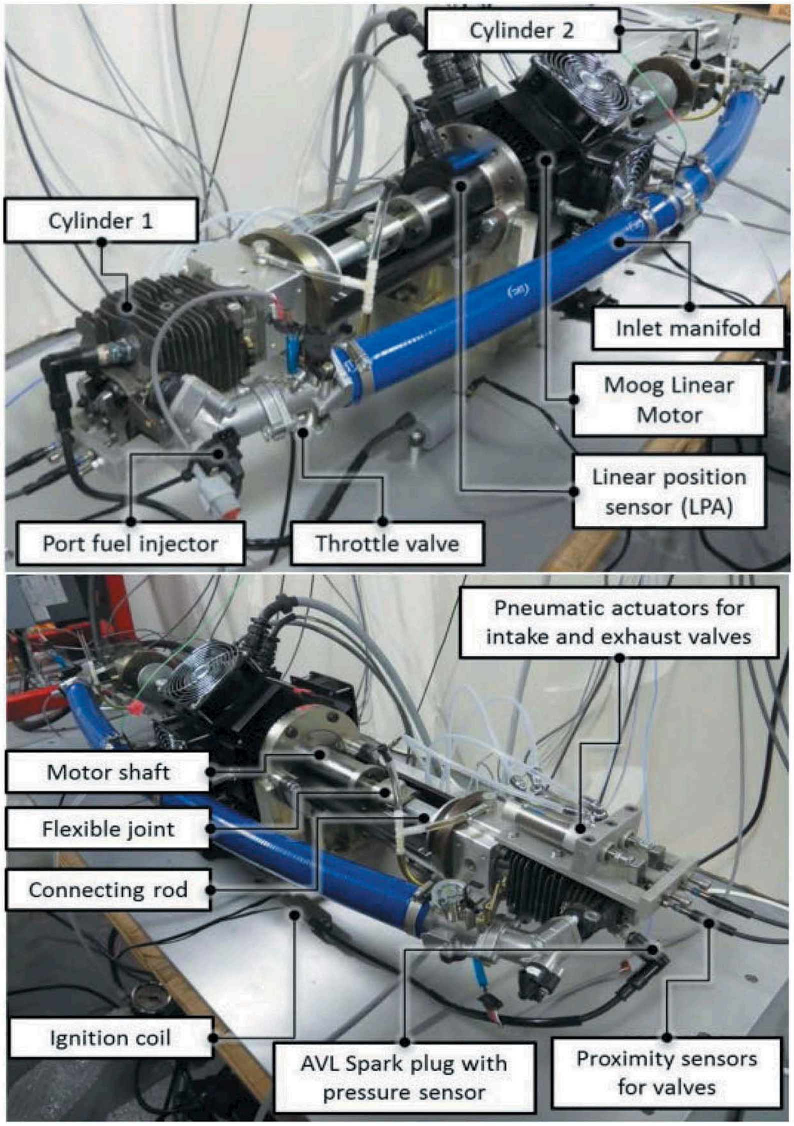

Figure 2. FPEG prototype.

2.2 Four-stroke and two-stroke control mode

To operate the FPE in four-stroke mode, each cylinder requires two oscillation cycles or four oscillatory motion of its piston to complete the sequence of operations that finishes a single power stroke. The processes of four-stroke cycle are as follows [17].

1) Suction/Intake stroke: During this stroke, the piston will be at its TDC and the valve control system opens the intake valve. This stroke is continuous as piston reaches to its BDC and ended by closing of intake valve. If there is not enough force behind the piston to drive this event then the electric machine acts as a motor.

2) Compression stroke: During this stroke, both the inlet/intake and outlet/exhaust valves are in closed positions and the piston compresses air–fuel mixture as it moves from its corresponding BDC to TDC. If there is not enough force behind the piston to drive this event then the electric machine acts as a motor. At the end of the compression stroke, the spark-plug produces the spark and initiates the combustion.
3) Power stroke: The combustion occurs at the end of compression stroke produces enormous amount heat energy with high pressure which pushes the piston towards its BDC. The kinetic energy of the piston movement is converted in to electricity by linear electric generator.
4) Exhaust stroke: This stroke initiated as the outlet valve opens and piston reciprocates from its corresponding BDC to TDC. The burnt gases expel out from the cylinder chamber and the cycle is repeated as outlet valve closes.

Similar with the working of FPEG in two-stroke mode, alternatively each cylinder gets the power stroke and throughout the generating process, the linear electric machine is functioned as generator. The processes of two-stroke cycle are explained as follows.

1) Compression stroke: Throughout this stroke, the valve control system of FPEG closes both the inlet valve and outlet valve. As the piston moves from BDC to its corresponding TDC, the fuel-air mixture is compressed in the cylinder. This will continuous until the system achieves its compression ratio. At the end of this stroke, spark plug produces the spark for the combustion.
2) Power stroke: The initiation of power stroke is determined by spark timing and expansion of combustion gases. Expanded gas pushes the piston from TDC to its corresponding BDC. The control system opens the outlet valve followed by inlet valve and the exhaust gas expel out from the cylinder and fresh air fuel mixture is enters the cylinder.

The Table 2 provides the sequence of processes in each cylinder and corresponding modes of linear machine operation for the four-stroke and two-stroke cycles. During four-stroke mode of engine operation, the linear machine switched to motor as well as generator according to strokes and it act as a generator throughout the two-stroke mode of engine operation.

Table 2. Sequence of processes of FPEG in two-stroke and four-stroke mode.

	Four-stroke			**Two-stroke**		
	Right cylinder	**Left cylinder**	**Linear machine**	**Right cylinder**	**Left cylinder**	**Linear machine**
Stroke$\longrightarrow$	Air exhaust	Air intake	Motor	Gas exchange + compression	Power + gas exchange	Generator
Stroke$\longleftarrow$	Air intake	Compression	Motor	Power + gas exchange	Gas exchange + compression	Generator
Stroke$\longrightarrow$	Compression	Power	Generator	Gas exchange + compression	Power + gas exchange	Generator
Stroke$\longleftarrow$	Power	Air exhaust	Generator	Power + gas exchange	Gas exchange + compression	Generator

2.3 Valve actuating mechanism

The designed FPEG is facilitated with a Festo pneumatic system to activate the overhead intake and exhaust valves. Nominally, the valve lift is 4 mm, though this is changeable, which permits for further control, improvement and optimization of the valve operation. To operate the FPEG in four-stroke mode, the valve control system opens inlet valve towards the end of exhaust stroke and closes at the end of suction stroke. This gives the maximum compression stroke of about 40mm. The outlet valve opens at the end of the power stroke and it remains open throughout the exhaust process. In two-stroke mode, the compression process starts after the closing of inlet valve which result in reduction of compression stroke to 34mm. The scavenging process of two-stroke mode of operation combines intake and exhaust gas exchange process. The poppet valves are used for both intake and exhaust processes rather than scavenging ports. During the process exhaust valve opens before opening of intake valve and it closes after the closing of intake valve. A compressor is employed in FPEG for the two-stroke mode of operation to enhance the manifold pressure and each outward stroke relates to a power stroke. As the valves are actuated based on the piston position, the scavenging durations for both operating modes will be significantly affected by the engine speed and piston profile. In order to avoid mechanical contact between the piston and cylinder head, the working mode of the linear electric machine is switched at a specific point during Stroke 1 and Stroke 2.

2.4 Numerical model description

The numerical model was built on many of the assumptions and principles of thermodynamic models employed regularly across the conventional ICE research and development community. A full description can be found elsewhere [11,13,14,15]. An engine dynamic model was formed to determine the piston motion. The three sub models of in-cylinder gas thermodynamic processes, linear electric machine force and mechanical friction force were developed and fed into the engine dynamic model. The in-cylinder gas thermodynamic process comprises heat transfer to the wall, piston's expansion or compression process, gas leakage, gas exchange process, scavenging process for two-stroke engine mode and heat release during combustion. The linear electric machine force considered is either resisting force or driving force depending on its operating mode whereas the friction sub model defines the friction force acting on the piston rings.

The model was developed in Matlab/Simulink. The developed model is used for both starting and steady operation of FPEG. In starting mode, the combustion model was disabled, and linear electric machine was enabled to run as a motor. In steady operation, the linear electric machine operates as a generator and combustion model was enabled. The computed piston velocity, in-cylinder pressure, and piston displacement at the end of the starting process were taken as the preliminary values for the steady operation of the FPEG.

The design parameters for the prototype and initial boundary conditions are fixed as the two and four-stroke mode of operations are employed on the same prototype. The considerable changes are the working mode of the electric machine and the valve timing strategy. The prototype specifications and the input parameters for both mode of engine operation is tabulated in Table 2.

3 RESULT AND DISCUSSIONS

3.1 Simulation results

The objective of the simulations was to identify different ways in which the engine could be controlled to achieve stable and steady operation. In doing so, it would become clearer as to what hardware would be required and how to control the system. The same analysis aimed to explore the sources of power losses in its operation and the sensitivity of these parameters on performance.

3.1.1 *Exploring engine operational performance*

The simulation of the FPEG engine was carried out at stoichiometric air–fuel ratio (λ=1.0) with the target piston dead centre is +17.0mm and -17.0mm from the middle position of the stroke and clearance from the cylinder head is 4.0mm. The engine performance of both four-stroke and two-stroke is shown in Table 3. The two operational modes were compared with the motor force shown in Table 1.

With a fixed motor force, it was noted the system operated at different engine speeds depending on the operating mode. Furthermore, the indicated power is much greater for two-stroke engine cycle compared to four-stroke engine mode of operation. The engine speed for the two-stroke cycle mode was higher, and the power stroke took place in every cycle. In the meantime, in four-stroke mode of operation, the peak cylinder pressure and the movement of the piston would produce higher friction between piston ring and cylinder liner interface. in overcoming. This results in almost half the indicated power is consumed in overcoming the friction along with the pumping losses of the motoring process.

Table 3. Predicted FPEG performance parameters in four and two-stroke mode.

Performance parameters	Four-stroke	Two-stroke
Mean speed (rpm)	900	2000
Operating Frequency (Hz)	15	31
Maximum piston velocity (m/s)	3.8	3.1
Maximum cylinder pressure (bar)	76	47
Thermodynamic efficiency (%)	44.9	34.5
Consumption of fuel (kg/kW h)	0.20	0.22
Indicated power (W)	1230	3900
Electric power output (W)	640	3760
Maximum compression ratio	16.2	7.36
Power to weight ratio (W/kg)	0.22	0.070

3.1.2 *Engine throttle position*

The Figure 3 demonstrates the effect of engine throttle opening positions on indicated power and electric power production. For two-stroke cycle, a reduction in indicated power from 5 kW to 1.8 kW is occurred when the throttle opening mode was changed from fully-open to half-open. In the interim, the electric power generation is somewhat lesser than the indicated power. It also observed that, with the same throttle opening positions, both indicated power and electric power of four-stroke cycle are considerably lesser than that of the two-stroke cycle. The indicated power decreases from 1.8 kW to 0.8 kW when the throttle opening area reduces from 100% to 50%. It is recommended to operate the engine at higher loads rather than below 50%, as the energy conversion efficiency is getting minimal for the four-stroke mode.

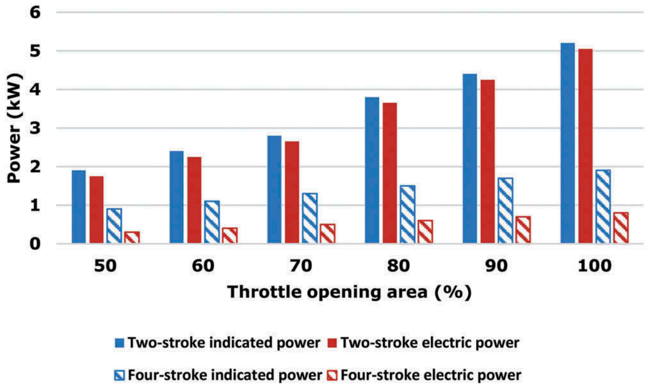

Figure 3. Variation of power with throttle opening area.

3.1.3 *Ignition timing*

Figure 4 displays the variations of indicated power with ignition timing for two-stroke and four-stroke engine mode when it runs at wide open throttle. As it can be seen from the plot, for the two-stroke engine mode, the electric power slightly increases with the increase in ignition timing. Advancing ignition timing can reduce the period of post combustion and improve the in-cylinder pressure. However, with the ignition timing advance, no substantial variation was detected neither in indicated power nor in electric power when FPEG is operated in four stroke engine mode.

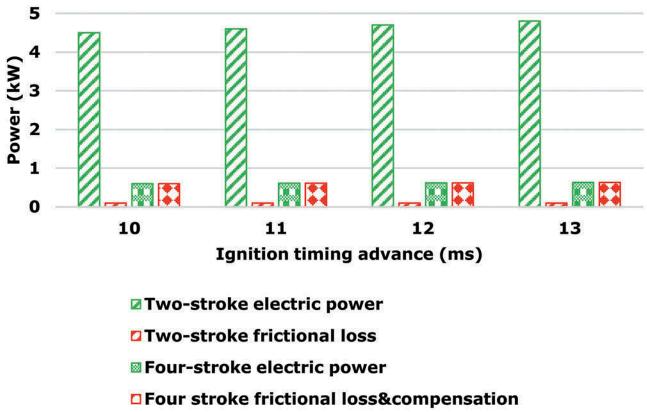

Figure 4. Variation of power with ignition timing.

3.1.4 *Power circulation*

Indicated power distributions in two and four-strokes cycle of FPEG when it runs at wide open throttle are depicted in Figure 5. As there is removal of crankshaft and connecting rod in the FPEG, it helps in the reduction of frictional losses as compared to conventional engines, which in-turn reduces the fuel consumption. Compensation is the electric power used to offset the overall power consumptions during the motoring process. Compensation was zero for two-stroke cycle and was 42% for four-stroke cycle, *i.e.* during the motoring processes for supplying additional electric power, 42% of the indicated power was consumed.

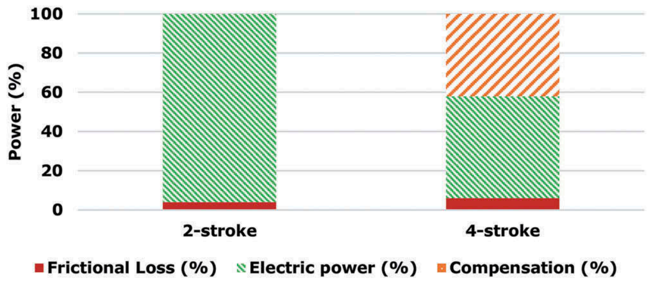

Figure 5. Power distribution in two-stroke and four-stroke cycle.

3.1.5 *Effect of motor force on power of four-stroke cycle*

During four-stroke mode of FPEG operation, the linear electric machine primarily acts as a motor and later as a generator. An important parameter for four-stroke cycle which influences on FPEG performance is the motor force. The Figure 6 illustrates the different motor force effect on FPEG's electric power, frictional loss and compensation at wide open throttle. As seen from the plot, the electric power increases with the increase of motor force. The higher motor force reduces the period between pumping and combustion which raises the engine speed and thus further development of indicated power. The plot also depicts that, as motor force increases, engine consumes more power to recompense the supply of electric power during motoring process.

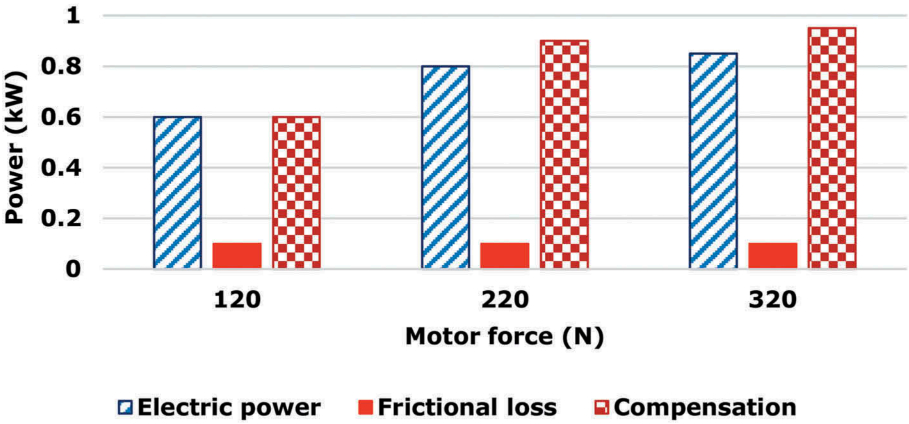

Figure 6. Power distribution with different motor force.

3.2 Experimental results

The numerical modelling indicated that manipulation of the motor force itself could be used to control the engine with a high degree of fidelity. As a result, the decision was made to utilise a more complex hardware and control system which could control the motor force in real time to achieve a sinusoidal motion profile at a pre-defined frequency.

3.2.1 *Control signals*

The experimental results of two-stroke mode of FPEG operated at 5Hz have been presented in this section. During suction phase of FPEG, the compressed air is supplied to the engine through an intake manifold to facilitate gas exchange and to boost the intake manifold pressure. Nominally, the engine was operated at stoichiometric air–fuel ratios (λ=1.0).

The timing of spark and valve opening/closing are initiated based on piston displacement and velocity. Figure 7 illustrates the control signals for the spark and valve timing for a cylinder of FPEG. The spark plug produces the spark to initiate the combustion before the piston reaches its TDC. The exhaust valve opens before opening of intake valve and intake valve closes after the closing of exhaust valve as seen in the diagram.

3.2.2 *Pressure and volume*

Variation of pressure and velocity with the displacement is depicted in Figure 8. In this figure, the obtained piston velocity curve is close to a sinusoid and pressure curve depicts the work done by the gas expansion. At the middle stroke of the piston, the highest velocity ensues, and value of velocities are zero at the dead centres where the value of velocity changes its sign.

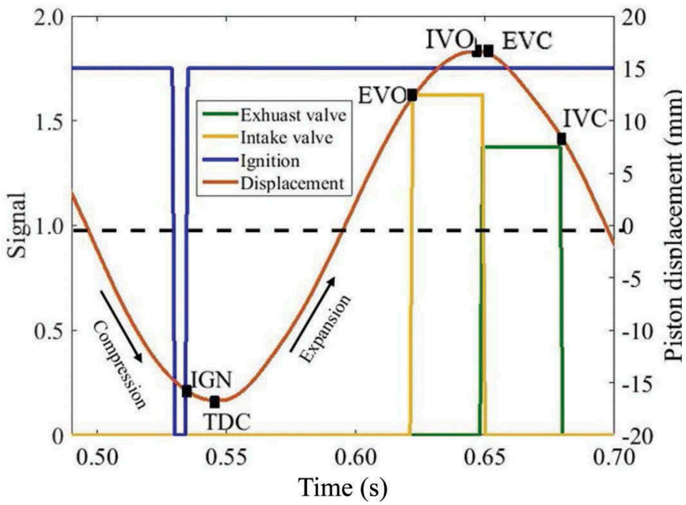

Figure 7. Control signals in a cylinder.

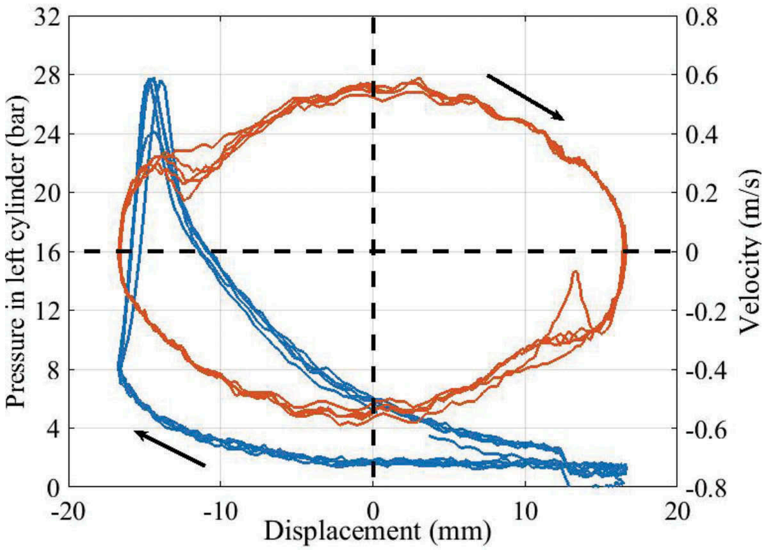

Figure 8. Cylinder pressure with displacement.

3.2.3 *Piston dynamics*

Figure 9 illustrates piston velocity and its displacement attained during the test. Figure represents the five separate compression and expansion events occurred in the engine. As expected, the value of piston velocity and displacement were increased. The profile typically achieves a ± 17mm displacement and the impact of combustion is more apparent in the plot.

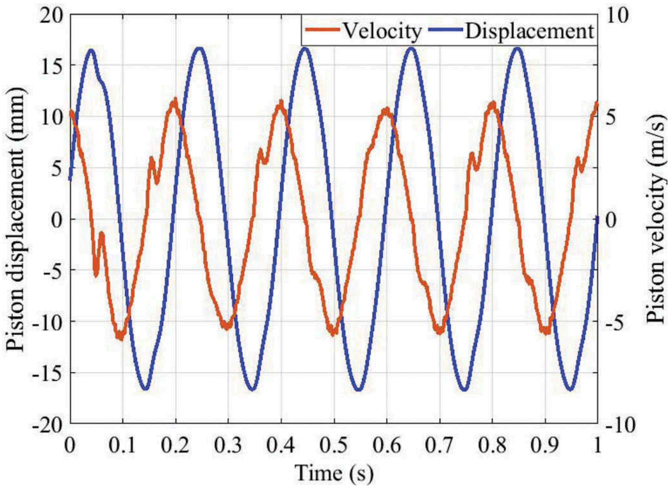

Figure 9. Piston dynamics.

3.2.4 *Cylinder pressure*

Variation of in-cylinder pressure for each cycle and its corresponding ignition signal with respect to time is shown in Figure 10. From the plot, it can be concluded that the in-cylinder pressures are rapidly increasing and decreasing when combustion occurs. The peak pressure of 27 bar attained by the engine cylinder during the combustion as seen from the plot.

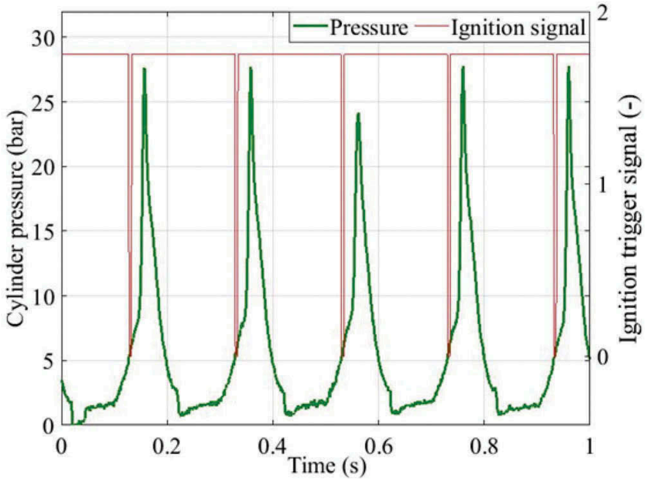

Figure 10. In-cylinder pressure.

3.3 Effect of intake and exhaust valve timings on IMEP

During the above testing, the engine was operating continually without issue. It was then considered that a parameter sweep would be carried out on valve timing. The objective being to explore the sensitivity of the system stability.

3.3.1 *Intake valve closure timing*

The duration of opening was fixed to 40 ms (milli-seconds) and the intake valve closing (IVC) timing set from -6 ms to +6ms aBDC (after Bottom Dead Centre). The results of variation of an intake valve closure (IVC) timing on indicated mean effective pressure (iMEP) are displayed in Figure 11.

As IVC timing is delayed, the in-cylinder pressure is reduced as less combustible mixture is trapped within the cylinder chamber in turn lowers the pressures at spark ignition. The reduced pressure of less amount of combustible mixtures produces lower indicated mean effective pressure as depicted in the plot.

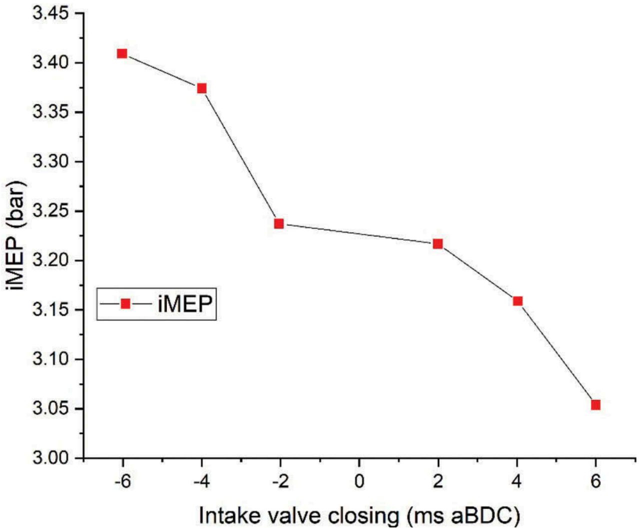

Figure 11. Effect of intake valve closure timing on iMEP.

3.3.2 *Exhaust valve opening timing*

The results of variation of an exhaust valve opening (EVO) timing on indicated mean effective pressure are presented in Figure 12. The open duration was fixed to 39 ms and EVO timing was varied from 33 ms to 39 ms aTDC (after top dead center).

Delaying the EVO generally resulted in higher in-cylinder pressures with later opening times. However, the Figure 12 shows only minor differences in iMEP with the variation of EVO timing. It was observed that beyond 33 ms to 39 ms EVO timing limits, the engine failed to operate with the combustion due to ineffective scavenging process.

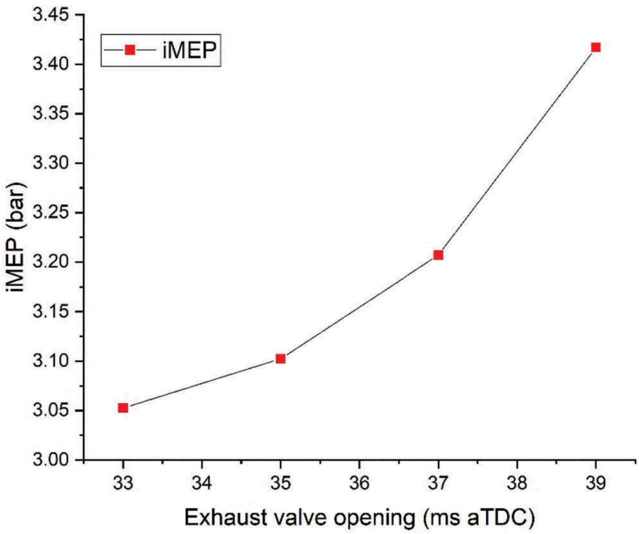

Figure 12. Effect of exhaust valve opening timing on iMEP.

4 SUMMARY

In the present study, the performances of two-stroke and four-stroke cycles of a FPEG are compared. The work can be summarised as:

- A novel twin-opposed free-piston engine prototype has been design, built and tested.
- A numerical model of the system has been developed which was used to understand and determine its core control algorithms
- Using the model, motor force was identified as a key control parameter able to ensure stable operation.
- The prototype was then upgraded to enable control of motor force in real time and thus to enable for the piston motion to follow a sinusoidal profile.
- The first experimental results showing operation of the prototype are presented and discussed.

REFERENCES

[1] R.P. Pescara, Motor compressor apparatus. US Patent 1,657,641, 1928.

[2] W.T. Toutant, The Worthington–Junkers free-piston air compressor, Journal of the American Society of Naval Engineers 64 (3) (1952) 583–594.

[3] C. Zhang and Z. Sun, "Trajectory-based combustion control for renewable fuels in free piston engines," Applied Energy, vol. 187, pp. 72-83, 2017.

[4] A. H. Roman Virsik, "Free piston linear generator in comparison to other range-extender technologies," World Electric Vehicle Journal, 2013.

[5] A. Heron and F. Rinderknecht, "Comparison of Range Extender technologies for Battery Electric Vehicles," in Eighth International Conference and Exhibition on Ecological Vehicles and Renewable Energies (EVER), Monte Carlo, Monaco, 2013.

[6] R. Huber, Present state and future outlook of the free-piston engine, Transactions of the ASME 80 (8) (1958) 1779–1790.

[7] Kosaka, H., Akita, T., Moriya, K., Goto, S., Hotta, Y., Umeno, T., and Nakakita, K. (2014). Development of Free Piston Engine Linear Generator System Part 1 - Investigation of Fundamental Characteristics. https://doi.org/10.4271/2014-01-1203

[8] Goto, S., Moriya, K., Kosaka, H., Akita, T., Hotta, Y., Umeno, T., and Nakakita, K. (2014). Development of Free Piston Engine Linear Generator System Part 2 - Investigation of Control System for Generator. https://doi.org/10.4271/2014-01-1193

[9] Mikalsen R, Roskilly AP. The design and simulation of a two-stroke free-piston compression ignition engine for electrical power generation. Appl Therm Eng 2008;28(5);589–600. https://doi.org/10.1016/j.applthermaleng.2007.04.009

[10 Hanipah, M. R., Mikalsen, R., and Roskilly, A. P. Recent commercial free-piston engine developments for automotive applications. Appl Therm Eng 2015;75; 493-503. https://doi.org/10.1016/j.applthermaleng.2014.09.039

[11] B. Jia, R. Mikalsen, A. Smallbone, A. P. Roskilly, A study and comparison of frictional losses in free-piston engine and crankshaft engines, Appl Therm Eng,140,217-224, doi:https://doi.org/10.1016/j.applthermaleng.2018.05.018.

[12] Hanipah, Mohd Razali. Development of a spark ignition free-piston engine generator. Diss. Newcastle University, 2015.

[13] Jia B, Zuo Z, Tian G, Feng H, Roskilly AP. Development and validation of a free-piston engine generator numerical model. Energy Conversion and Management. 2015 Feb 1;91:333-41.

[14] Jia B, Mikalsen R, Smallbone A, Zuo Z, Feng H, Roskilly AP. Piston motion control of a free-piston engine generator: A new approach using cascade control. Applied energy. 2016 Oct 1;179:1166-75.
[15] Jia B, Smallbone A, Zuo Z, Feng H, Roskilly AP. Design and simulation of a two-or four-stroke free-piston engine generator for range extender applications. Energy conversion and management. 2016 Mar 1;111:289-98.
[16] Mikalsen Rikard, Roskilly AP. Free-piston internal combustion engine. U.S. patent application 13/698,569.
[17] Heywood JB. Internal combustion engine fundamentals. McGraw-Hill Press. 1988.